Journal Name

Dynamic Article Links ►

Cite this: DOI: 10.1039/c0xx00000x

www.rsc.org/xxxxxx

ARTICLE TYPE

Chameleon-like Behaviour of Cyclo[n]paraphenylenes in Complexes with C_{70}. On Their Impressive Electronic and Structural Adaptability as probed By Raman spectroscopy.

Juan Casado

Received (in XXX, XXX) Xth XXXXXXXXX 20XX, Accepted Xth XXXXXXXXX 20XX
DOI: 10.1039/b000000x

A series of four 1:1 host-guest supramolecular complexes of [n]CPPs and C_{70} have been analyzed by Raman spectroscopy in solid state and complemented with the analysis of their spectroscopic responses under mechanical and thermal stresses. By following the frequency behaviour of the G and RBM modes we have found that [10]CPP in the [10]CPP@C_{70} complex displays a more "ordered" structure. However, in [11]CPP@C_{70}, the nanoring gets ovallized with closer contacts with the C_{70} poles and less conformational restriction in the flattened region. By mechanical and thermal stresses we are able to modify the lying conformation of [10]CPP@C_{70} towards a standing shape. [11]CPP@C_{70} resists pressure changes, although it tends to shift from the standing to the lying orientation by heating. As for the crystal cell, the [n]CPPs occupy the residual empty spaces while the main crystallographic positions are reserved to C_{70}. These are new examples of the impressive adaptability of the [n]CPP molecules to different physico-chemical environments, a chameleon-like property which reveals the delicate equilibrium provided by cyclic conjugation and ring strain.

A Introduction

Cyclo[n]paraphenylenes (abbreviated as [n]CPP, see Figure 1) are a class of conjugated pure-hydrocarbon molecules featured by a cyclic disposition of 1,4 substituted benzenes with the p_z carbon orbitals oriented towards the macroring center. Given their aesthetic shape, they attracted the interest of chemists for a long time.[1] It was in 2008 when Jasti and Bertozzi[2] were able to synthesize cyclo[n]paraphenylene compounds, for the first time, [8]CPP, [12]CPP and [18]CPP, paving the way for the preparation of [n]CPP of almost all sizes, [6]- to [18]CPP, in a beautiful competition race mainly between the groups of Itami[3], Yamago[4] and Jasti[5]. Very recently, the smallest member of the series, [5]CPP, has been successfully prepared almost simultaneously by Yamago and Jasti.[6]

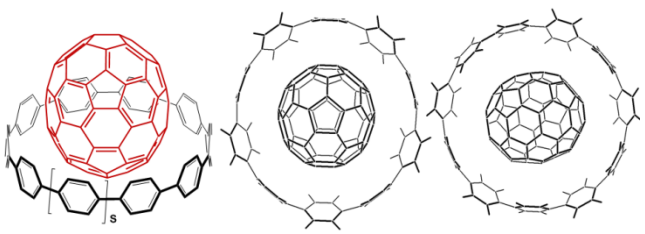

Figure 1. Left: Chemical structures of the [n]CPP compounds (s=0 for [9]CPP, s=1 for [10]CPP, s=2 for [11]CPP and s=3 for [12]CPP). Middle: lying disposition for [10]CPP@C_{70} and standing disposition for [11]CPP@C_{70}.

The analogy between [n]CPPs and armchair single wall carbon nanotubes (SWCNT) is straightforward: the [n]CPP can be considered as the shortest version of arm-chair SWCNTs and, as such, can be considered as their molecular models. While the chemical undefinition of SWCNTs is a insurmountable obstacle for the full understanding of their properties, the perfect knowledge of the chemical structures of the [n]CPP series allows to evaluate the evolution of their electronic, structural and optical properties as a function of the [n]CPP size thus permitting the first *oligomeric approach* to the physical properties of SWCNT. But [n]CPPs have been also used as templates for the chemical synthesis of SWCNT via a controlled vertical condensation of [n]CPP, as reported by Itami,[7] which supposed the first successful preparation of nanotubes by using an orthodox synthetic organic approach. On their own way, the [n]CPPs display very interesting optoelectronic properties as well thanks to the co-existence of rather unusual effects such as molecular strain and cyclic conjugation. Cyclic strain increases with the decrease of the number of benzenes[8] and produces in these rings some slight deformations from planarity and their partial benzo-quinonoidization.[9] On the other hand, cyclic conjugation, which is provided by these p_z orbitals contained in the circumferential molecular plane, further stabilizes the whole cyclic arrangement. As a result, these appealing molecules contain highly polarisable electronic shapes in the belt which originate other interesting chemical properties such as the ability to form host-guest π–π and van der Waals supramolecular complexes. These complexes are the focus of this article.[10]

We have recently reported on the dependence of the structural and electronic properties of the [n]CPPs (from [6]CPP to [12]CPP) with their size, and established robust relationships between quinonoidization, cyclic strain, cyclic conjugation and [n]CPP dimension, using Raman spectroscopy as the revealing tool.[11] Another structural feature of significance is their conformational effect that makes these [n]CPPs to be irregular cylinders with the successive benzenes canted or staggered with opposite angles.[8,9] We have also addressed the structural flexibility of the whole nanohoop which, for the larger

compounds, are able to undergo reversible ovallisation under strong mechanical stress.[11] The ability to readapt their shapes, their inner empty cavity, and the capacity to promote favourable surrounding π–π electronic interactions, are the basis for the formation of the 1:1 stoichiometric complexes.[10]

In this paper, we go a step further on these studies of [n]CPPs and address in detail the conformational and electronic effects of new [n]CPP complexes with a new guest, such as C_{70}.[12] The oval shape of this fullerene will allow us to get new insight of the connection between [n]CPP shape, its conformational plasticity and the electronic properties of the formed complexes. The whole study will be carry out by using Raman spectroscopy as the structural and electronic diagnostic tool. Raman spectroscopic properties will be investigated as a function of mechanical stress (pressure dependent measurements) and thermal stress (temperature dependent measurements). With this study we aim to provide new features of the particular physical and chemical properties of [n]CPP resulting from their impressive propensity to reshape their structures.

B Experimental Procedures and technical Details

The syntheses of the [n]CPP and of their complexes with C_{70} have been published elsewhere.[12] The samples were studied as pure solids, and these were well characterized by different analytical and crystallographic techniques.

Raman measurements were carried out with a Senterra dispersive micro-Raman spectrometer from Bruker with a 785 nm laser as the excitation. The Raman scattering radiation was collected in a back–scattering configuration with a standard spectral resolution of 3 cm^{-1}, a spatial resolution of 0.5 μm, and a spot size of about 3 μm.

High pressure studies were conducted in a sapphire anvil cell (SAC) with a diameter culet of 400 μm and a gold gasket.[13,14] No pressure transmitting medium was used and diamond chips were placed as the pressure calibrant. The Raman experiments were carried with the same Senterra microscope with 785 nm laser excitation. The recovered samples, after pressure cycles, were also analyzed, taking several spectra on different sample points to confirm the reproducibility on the same sample and to ensure whether the transformation of the samples is complete or not.

Laser excitation time dependent measurements were carried out in the micro-Raman spectrometer (BWTEK Voyage™ BWS435-532SY) with an excitation wavelength of 532 nm. These experiments were repeated at different temperatures ranging from 298 to 523 K. The [8]CPP sample was placed in a Pt crucible and situated inside the high temperature stage system (Linkam TS1500 with a T95 system controller). This system can heat within a temperature range from ambient up to 773 K, allowing us to observe and characterize samples through its quartz lid window. The high temperature stage system was equipped with a Pt/Rh thermocouple in direct contact with the ceramic heating element to detect and control the sample temperature. During the experiments, the temperature was stabilized within ± 0.1 degrees. It was necessary to wait between 10 and 15 minutes for the sample to have a uniform temperature. Variable temperature Raman experiments on the complexes were carried out in the same Linkam TS1500 device but the excitation laser used was the 785 nm of the Senterra dispersive micro-Raman spectrometer from Bruker.

C Vibrational Raman Antecedents on [n]CPPs.

The Raman spectra of [n]CPPs are characterized by the existence of four main Raman bands which constitute the fingerprint of their structure and electronic shapes.[11] For our discussion in this paper we will focus only in two: i) the strongest band of the spectrum at 1580-1600 cm^{-1} which corresponds to the analogue G mode in SWCNT (in our [n]CPP we call it as G mode as well) and is described as a CC stretching mode along the tangential direction of the tube. This G mode is composed of two sub-bands the so called G_1 and G_2 modes. The frequency of the G_1 band in the [n]CPPs has been related with the degree of quinonoidization of the benzene units due to the cyclic strain. And ii) the pseudo-radial breathing modes in our [n]CPPs which is related with the radial breathing vibrational mode of SWCNTs, a molecular motion that takes place along the radial direction of the tube and appears in the 400-100 cm^{-1} range. From a structural-spectroscopy relation, the frequency of this `pseudo-RBM band is quite sensitive to the cyclic radius (therefore size) of the [n]CPP.

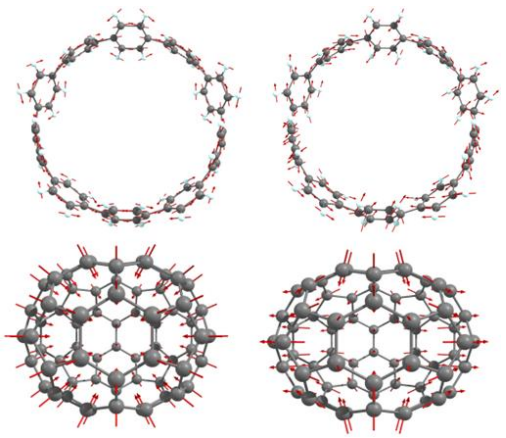

Figure 2. Top: vibrational modes associated with the G_1 band of [10]CPP (left) with its pseudo radial breathing mode (right) from reference 11. Bottom: radial breathing mode (left) and radial-like breathing mode (right, squashing mode) of C_{70}, in the experimental spectrum these modes are observed at 456 and 256 cm^{-1}, respectively.

It is interesting to note the nature of the main Raman bands of the Raman spectrum of C_{70}, or those at: i) 1564 cm^{-1} which is due to a tangential CC stretching mode or G-like mode; ii) 456 cm^{-1} which is the radial breathing mode with has slightly more vibrational amplitudes along the *long* axial direction of the ellipsoid. And iii) 256 cm^{-1} which also corresponds to a sort of breathing radial-like mode (squashing mode) featured by main vibrational amplitudes in the atoms placed in the equatorial segment of C_{70}.[15] Figure 2 depicts the normal modes associated to most of these relevant bands.

D Conformational studies.

In this section we will address the analysis of the conformational properties of the [n]CPP as individual entities with the objective of understanding them before the CPP assemblies with C_{70} fullerene. To this end, we have studied the effect that simultaneous thermal and laser excitation stresses cause on the [n]CPP spectra. Figure 3 shows the time evolution of

the Raman spectra of [8]CPP, as a prototypical example, at 25 ºC by exciting with the 2.33 eV laser. It must be indicated the same experiments with low energy Raman excitation at 1064 nm did not produce any spectral change.

Figure 3. 532 nm Raman spectra of [8]CPP. a) Deconvoluted spectrum at initial time and at 298 K; b) Deconvoluted spectrum recorded after exposition time at the laser radiation of about 300 min at 298 K. Middle: Ratio between the area of the 1604 cm^{-1} band and the area total of these features as a function of the exposition time at the laser radiation at several temperatures. Right: representation of the ring rotation with its energy barrier.

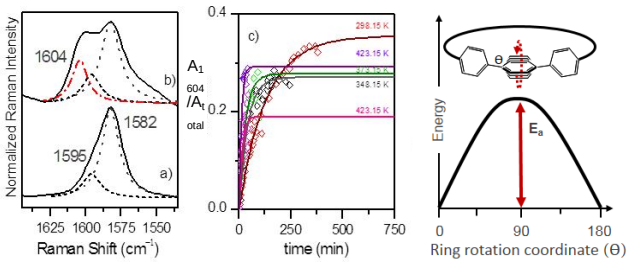

Changes in the spectra are clearly visible resulting in a new peak at 1604 cm^{-1}. The time growth of the integrated area of this band (relative to that at 1582 cm^{-1}) allows us to obtain the rate constant for the process which studied as a function of the temperature gives us the activation barriers associated with the conversion towards the structure responsible for the new Raman component. For the growth of the 1604 cm^{-1} band a value of E_a = (19.9 ± 1.3) kJ/mol is determined. This activation energy is different depending on the [n]CPP size, for instance, in [12]CPP the strongest 1594 cm^{-1} band also evolves into the new band at 1604 cm^{-1} with a value of E_a = (22.0 ± 2.0) kJ/mol.[8,9] These experimental activation energies are in excellent agreement with those energy barriers calculated for the full rotation of a given benzene regarding their vicinal rings around the inter-ring C-C bonds. As a result, the energy barriers for the conversion into a species with a new band up-shifted (1604 cm^{-1} bands) regarding the original ones is in consonance with the transformation into a more distorted or staggered conformation among the successive rings of the cycle, where these barriers might be viewed as the maximal energy costs for full rotation (Figure 3). We speculate that the need of assistance by high energy radiation to develop the conformational effect can be explained by the formation after light absorption of an excited state closely related with the transient state for this internal rotation.

E Complexation of [n]CPP with C_{70}: the 1:1 complexes.

On the interpretation of the G modes of the [n]CPP. Figure 4 and 5 display the Raman spectra of the 1:1 complexes, [10]CPP and [11]CPP; [9]CPP and [12]CPP, respectively, The solid state structures of [10]CPP and [11]CPP have been fully characterized by x-ray diffractometry in solid state and by UV-Vis electronic absorption spectroscopy in solution.[12] For the shorter and larger complexes, no crystallographic data are available. To a first sight, in comparison with the respective [n]CPP, complexation induces much larger changes on the Raman spectra of [10]CPP and [11]CPP compared to those of [9]CPP and [12]CPP.

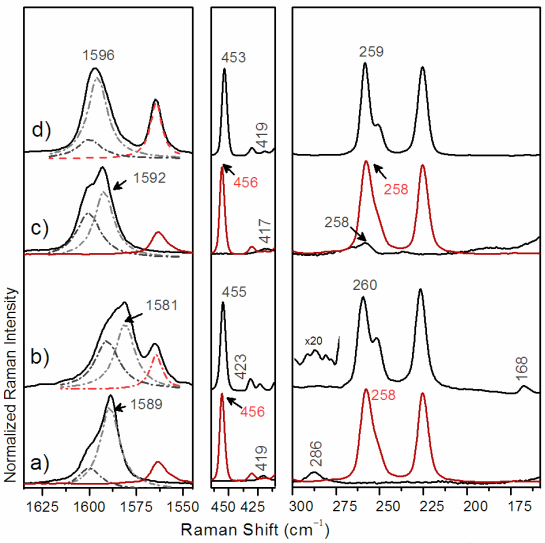

Figure 4. Solid state 785 nm Raman spectra at 25ºC of: a) [10]CPP (black) and C_{70} (red); b) [10]CPP@C_{70}; c) [11]CPP (black) and C_{70} (red); d) [11]CPP@C_{70}. Dashed lines correspond to the deconvoluted bands.

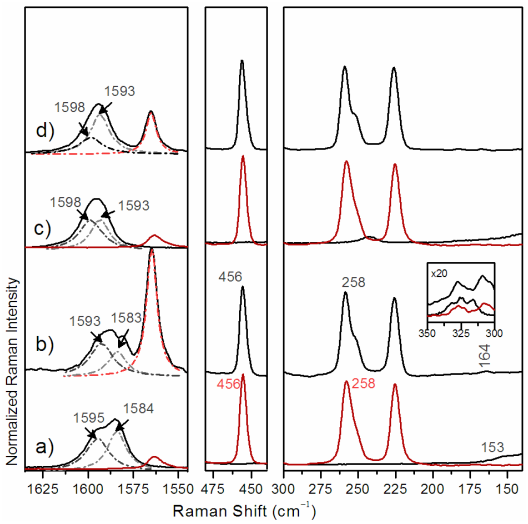

Figure 5. Solid state 785 nm Raman spectra at 25ºC of: a) [9]CPP (black) and C_{70} (red); b) [9]CPP@C_{70}; c) [12]CPP (black) and C_{70} (red); d) [12]CPP@C_{70}. Dashed lines correspond to the deconvoluted bands.

For [10]CPP@C_{70}, the G_1 mode frequency of [10]CPP changes from 1589 cm^{-1} to 1581 cm^{-1} in the complex. We have previously assigned the downshift behaviour of the G_1 band in [n]CPP to the quinonoidization effect of the benzene rings that simultaneously brings the formation of less staggered structures between successive benzene rings (this effect is called below as a "ordering" effect in the belt). A decrease in the number of benzene rings producing more effective cyclic conjugation gives also rise to a more quinonoid less staggered alternating ring sequences. A clear example of the connection between Raman downshifts and quinonoidization is shown in the oxidation of a given cycloparaphenylene compound to its radical cation.[11] Therefore, the –8 cm^{-1} downshift of the G_1 band on [10]CPP →[10]CPP@C_{70} can be attributed to the "ordering" effect on the cycloparaphenylene structure as a result of the template effect that the C_{70} fullerene exerts on it mediated by the attractive π–π forces established between both compounds in the complex. Solid state studies on [10]CPP@C_{70} reveals that the C_{70} fullerene

occupies the internal cavity of the cycloparaphenylene with the CPP belt surrounding the shortest axis or equatorial segment of the fullerene ellipsoid, or *lying* disposition (see Figure 1).[12] The size of this short axis of C_{70} is 0.712 nm which compared with the diameter of [10]CPP, 1.380 nm, anticipates a favourable interaction between the two units with very suitable 0.33 nm van der Waals distances. As a result of the interaction on the circular equator, [10]CPP does not deform its cyclic shape which, together with the better alignment of the consecutive rings (lower torsional angles than in the pristine molecules) favour cyclic electron delocalization originating the Raman downshift.

The Raman behaviour in the case of the [11]CPP@C_{70} complex is different. The G_1 band, at 1592 cm^{-1} in the individual [11]CPP, upshifts to 1596 cm^{-1}, by +4 cm^{-1}. Contrarily to the case of [10]CPP@C_{70}, we should associate these changes also to the conformational effect, but in this case caused by a more staggered benzene ring distribution in the cycloparaphenylene (higher torsional angles between neighbouring benzenes). We have also shown that the formation of this more inter-ring distorted shape induces the diminishing of the quinoidal character, reverting towards a more aromatic form, justifying the upshift of the G_1 band. The size of the C_{70} long axis is 0.796 nm while the [11]CPP diameter is 1.51 nm, thus it anticipates the two structures will interact by van der Waals interactions along the long C_{70} axes. Indeed, the solid state structure of [11]CPP@C_{70} has been resolved in which, C_{70} adopts a *standing* conformation (see Figure 1) where the maximal coupling is through the two poles of C_{70} with the CPP rings of the belt all residing along the long axis of the ellipsoidal fullerene (this contrasts with the coupling through the equatorial part in [10]CPP@C_{70}).[12] As a result of this disposition, the [11]CPP undergoes a deformation of the cylindrical shape towards a more ellipsoidal flattened form. This description is nicely in agreement with: i) Our previous publication[11] where we have described the great flexibility of the CPP compounds in a series of detailed studies as a function of variable pressure. We have shown that by applying mechanical stress to the samples these reversibly deformed into oval or flattened shapes. This mechanical deformation was followed by Raman spectroscopy which probed a frequency up-shift, in two linear regimens, with the increment of pressure such as observed here for the same G modes on [11]CPP → [11]CPP@C_{70} ; ii) One can also argue that in order to stabilize the standing conformation the benzenes placed in the equatorial side, given its unsuitable disposition for π–π coupling, would prefer to slightly rotate in order to promote energetically favourable hydrogen-C_{70} or H⋯π interactions[16] what might result again in a more staggered disposition for these benzenes also contributing to the Raman up-shift. This explanation would support an increment of entropy in the complexation reaction regarding the [11]CPP and C_{70} reactants, such as deduced experimentally, thus allowing to understand the entropy controlled regime for the exergonic formation reaction of this complex.[12]

On the interpretation of the [n]CPP RBMs. The low frequency region 500-100 cm^{-1} of the Raman spectra of the [n]CPPs is important since the presence of the pseudo-RBM modes (see Figure 2) whose frequencies also account for the alteration of their donut-like cylindrical shape with the formation of the complexes in solid state. In [10]CPP and [11]CPP the pseudo-RBMs were assigned to the bands at 286 cm^{-1} and 258 cm^{-1} respectively, while the RBM modes were not detected in their Raman spectra.[11] After formation of the complexes, in the low frequency region, the spectra are clearly dominated by the C_{70} Raman bands which mostly mask the Raman fingerprint of the cycloparaphenylene unit. In despite of this, three main findings need to be mentioned: i) the pseudo-RBM modes, which seemingly disappear after complexation; ii) In [10]CPP@C_{70} a completely new feature appears in the spectrum at 168 cm^{-1} ; and iii) in the region around 500-400 cm^{-1} there is a band at 423 cm^{-1} in [10]CPP@C_{70} which evolves from the [10]CPP one at 419 cm^{-1} and at 419 cm^{-1} in [11]CPP@C_{70} from that at 417 cm^{-1} in [11]CPP. It seems that the interaction in the complex drastically alters the dynamics of the pseudo-RBM modes provoking their disappearance. Simultaneously the same electronic effect might give extra-intensity to the formerly weak (undetectable) RBM modes which emerges in the complex at 168 cm^{-1} (in the individual [n]CPP this mode would be expected to appear below 150 cm^{-1}). It might be argued that the slight symmetrical compression of [10]CPP around C_{70} could provoke a slight reduction of its diameter and, as a consequence, an increase of the RBM frequency given the reciprocal relationship between the RBM frequency and the diameter of the cylinder. Similar reasons can account for the frequency upshifts of the 430-400 cm^{-1} bands from the unperturbed CPPs.

On the interpretation of the C_{70} fullerene modes. Complexation has a much smaller impact in the Raman frequencies of the C_{70} fullerene given its rigidity which contrasts with the elasticity of the CPPs. However, there are two interesting features in the spectra of the complexes compared to that of C_{70} alone: i) the analogue radial breathing mode of C_{70} at 456 cm^{-1} (main atomic displacements lie along the long axis and on the poles of the ellipsoid, see Figure 2) changes by −1 cm^{-1} in [10]CPP@C_{70} and by −3 cm^{-1} in [11]CPP@C_{70}, the latter being the greatest in agreement with the formation of the standing complex where the strongest interaction between [11]CPP and C_{70} goes through these polar regions of the ellipse; and ii) another radial breathing mode of the C_{70} is that at 256 cm^{-1} (squashing mode, with main atomic displacements on the equator of the ellipse, see Figure 2) which appear at +2 cm^{-1} in [10]CPP@C_{70} and at +1 cm^{-1} in [11]CPP@C_{70}, the former being the greatest in agreement with the formation of the lying complex where the strongest interaction between [10]CPP and C_{70} goes through the equatorial belt of the fullerene. These are remarkably observations, since in SWCNTs peapods of C_{70}, not significant observations have been achieved on the C_{70} orientation changes along the CNT, due mainly to the lack of diameter, and thus of conformational, purity on the CNTs samples. However, it is straightforward that C_{70} it is vibrational affected by its orientation inside the tube cavity, as observed on CPPs.

The spectra of [9]CPP@C_{70} and [12]CPP@C_{70}. Their Raman spectra in Figure 5 display small, but appreciable, differences regarding the superposition spectrum of the individual components. In spite of that their innermost cavities are either small or large to accommodate C_{70} ([9] and [12]CPP have diameters of 1.23 nm and 1.66 nm, respectively), the differences in the spectra seem to indicate some new insights. The G_1 and G_2 bands at 1584 cm^{-1} and 1595 cm^{-1} in [9]CPP move to 1583 cm^{-1}

and 1593 cm^{-1} in [9]CPP@C_{70}. Such as in the [10]CPP @C_{70}, this downshift emerges from a less inter-ring staggered conformer, resulting from the template-ordering effect of C_{70} on the [9]CPP shape. The C-C tensile modes of C_{70} fullerene are all upshift by 1-2 cm^{-1}. Although the internal volume of [9]CPP is unable to accommodate the C_{70} fullerene, it could be thought in a partial encapsulation, possibly through one of the two poles or through the corannulene segments of the fullerene "egg", forming a proto-complex. Due to the formation of this pseudo-complex, a new RBM band at 164 cm^{-1} (from that at 153 cm^{-1} in [9]CPP) is detected. Simultaneously, the C_{70} RBM bands (456 cm^{-1} and 256 cm^{-1}) change both by +0.5 cm^{-1}. The changes in the Raman spectrum of the [12]CPP@C_{70} from its components are certainly smaller in accordance with the mismatch of their relative sizes for the stabilization of any persistent concave-convex interaction in the internal cavity of the cycloparaphenylene.

F Spectral responses of the [10]- and [11]CPP@C_{70} complexes under thermal and mechanical stresses.

Variable pressure Raman experiments. Figure 6 and 7 display the Raman spectra of [10]CPP@C_{70} and [11]CPP@C_{70} under pressure and on heating. Both thermal and mechanical treatments lead to rather different behaviour such as it will be discussed in continuation.

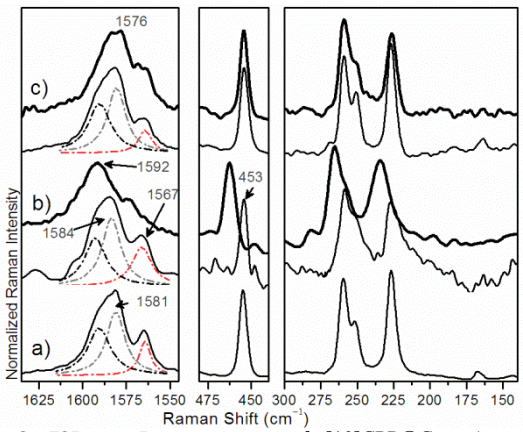

Figure 6. 785 nm Raman spectra of [10]CPP@C_{70}: a) at room temperature and pressure; b) thick black line corresponds to the spectrum at high pressure (≈ 2.0 GPa) and thin black line corresponds to the recovered spectrum after pressure cycle; both spectra taken at 25 ºC; c) thick black line corresponds to the spectrum at high temperature (140 ºC) and thin black line corresponds to the recovered spectrum after thermal cycle. Both spectra are taken at room pressure. Dashed lines correspond to the deconvoluted bands.

The application of pressure to [10]CPP@C_{70} induces an overall upshift of the whole spectrum together with the typical spectral broadening as exerted by the increment of the intermolecular contacts in the pressed sample. The G_1 band upshifts from 1581 cm^{-1} at room pressure to 1592 cm^{-1} at 2GPa, a significant shift which might be justified, not only because of the increasing frequency effect of pressure, but also because of the additional flattening of the [10]CPP structure towards a more oval shape.[11] This change is accompanied by a similar +12 cm^{-1} displacement (from 1564 cm^{-1} at room pressure to 1576 cm^{-1} at 2 GPa) of the tangential CC stretching mode of fullerene. The C_{70} bands associated to the RMB modes also experience big upshifts such as displayed in Figure 6. After pressure release the spectrum does not recover its original aspect, hence the G_1 band maximum is at 1584 cm^{-1} while the C_{70} tangential mode band is displaced to 1567 cm^{-1}.

In the case of the [11]CPP@C_{70}, the application of pressure again produces an upshift of its G mode frequency from 1596 cm^{-1} to 1603 cm^{-1} which is smaller than in [10]CPP@C_{70} (+11 cm^{-1}) corroborating the connection between frequency up-shifts and structural flattening as this varies from sample to sample. The smaller change in [11]CPP@C_{70} comes from the fact that the [11]CPP structure is already partially flattened in the standing complex at room pressure so that the space for further deformations is smaller. This could be due to the fact that the π–π contacts in the molecular region around the equatorial segment are not optimal leaving the possibility of a further ovallization. Similarly to [10]CPP@C_{70}, the C_{70} fullerene bands undergo ≈+10 cm^{-1} frequency displacements with pressure. The back to room pressure spectrum has suffered significant downshift on the CPPs' G bands, confirming the formation of a more staggered form to achieve better π–π contacts with C_{70}, but the low frequency C_{70} remains as in the pristine complex indicating the prevalence of the complex in its standing orientation.

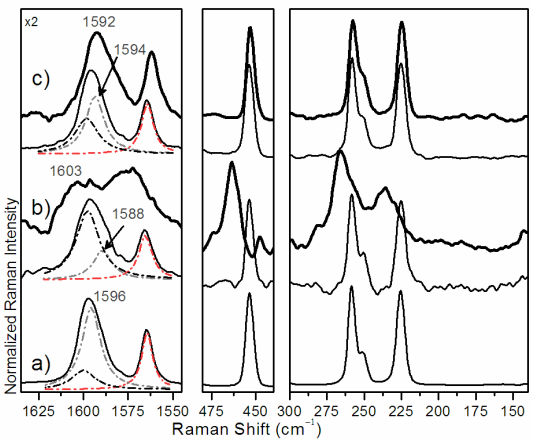

Figure 7. 785 nm Raman spectra of [11]CPP@C_{70}: a) at room temperature and pressure; b) thick black line corresponds to the spectrum at high pressure (≈ 2.0 GPa) and thin black line corresponds to the recovered spectrum after pressure cycle, both spectra taken at 25 ºC; c) thick black line corresponds to the spectrum at high temperature (140 ºC) and thin black line corresponds to the recovered spectrum after thermal cycle. Both spectra are taken at room pressure. Dashed lines correspond to the deconvoluted bands.

The fact that [10]CPP@C_{70}, does not recover the original aspect would be indicating that the [10]CPP could have slightly rotated from the lying disposition towards a situation closer, not identical, to the standing form. After pressure release this high pressure structure would result in a meta-stable kinetically blocked form. Figure 8 represents the evolution of the main Raman band frequencies of [10]CPP@C_{70} with pressure. In general, the G bands of the cycloparaphenylenes follow a different variation pattern compared to that of fullerene. These G bands of [10]CPP linearly shift up to a critical pressure, 0.6 GPa, at which they stay constant with the increment of pressure up to 1.6 GPa from which a second linear region is detected. However, the tangential CC stretching mode of fullerene follows a continuous linear regime in the whole range of pressure. This behavior on the cycloparaphenylene fragment could be related

with a re-orientational effect from the lying to standing shape in the first linear regime, while for the second linear segment, at higher pressures, the CPP undergoes a flattening process. The existence in the recovered spectrum of an upshift (from 1581 cm^{-1} to 1584 cm^{-1}) tells us about the reorientational movement in the complex which is the same effect found on going from a lying form in [10]CPP@C_{70} (1581 cm^{-1}) to the standing shape in [11]CPP@C_{70} (1592 cm^{-1}). In addition, the combination of both effects, reorientation plus flattening, imparts the observed irreversibility of the whole cycle. In the case of [11]CPP@C_{70}, the differentiation of the two frequency-pressure regimes is much less clear and the almost continuous behaviour before and after 1 GPa should be related with the predominance of the flattening process in the whole cycle process.

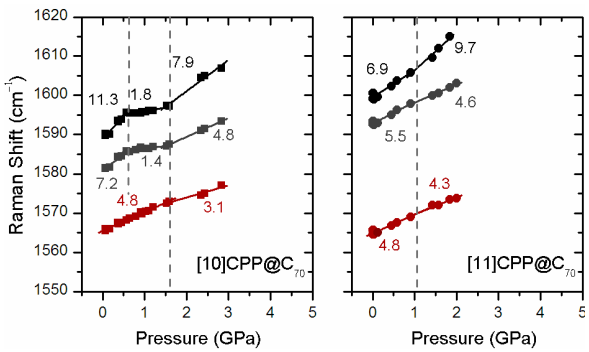

Figure 8. Evolution of the Raman frequencies of the G modes of the [10]CPP@C_{70} and [11]CPP@C_{70} samples as a function of pressure. Inserted values correspond to the pressure coefficients of each linear trend expressed in units of $cm^{-1}GPa^{-1}$. Black and grey dots correspond to the G_1 and G_2 bands of the [n]CPPs, respectively, while red points correspond to the 1565 cm^{-1} band of C_{70}.

The second aspect of relevance is that while from complex to complex at room conditions the main Raman spectral changes are observed for the CPP bands, here in the experiments at variable pressure, the C_{70} fullerene frequencies are those mainly altered. This could reveal that in the solid the relevant crystallographic positions are occupied by C_{70} while the [n]CPPs might mostly fill the empty space among them resulting that the main transmitters of the pressure in the solid are the C_{70} molecules which thus undergo the greater frequency changes.

These changes of the Raman frequencies of the [n]CPP in the complex by pressure in terms of re-orientational and flattening arguments are in agreement with the Raman data on the literature reported for analogous binary systems of C_{70} inside SWCNTs, or peapods.[17,18]

Variable temperature Raman experiments. Figure 4 and 5 also display the spectra within the thermal stress cycle. The spectrum of [10]CPP@C_{70} at 140 ºC is slightly different to that at room conditions, with the G band displaced –2 cm^{-1}. The formation process of this complex is exothermic meaning that heating would produce the rupture of the interaction in the complex leading to exactly the inverse effect of the G frequencies. Thus we argue that temperature only imparts a bulk effect with not affectation of the molecular structure of the complex, an interpretation corroborated by the spectrum back to room temperature which is exactly identical to the original one. In contrast, for [11]CPP@C_{70} it turns out that the G mode band is scarcely changed at 140 ºC (–0.5 cm^{-1}) while the recovered spectrum at room temperature shows the G band at 1592 cm^{-1}, which is unexpectedly similar to that of [11]CPP alone, 1592 cm^{-1}. A possible explanation is that heating would rotate the cycloparaphenylene from the standing situation towards the lying around the equatorial belt of the fullerene where the π–π distances increase, the π–π interaction is apparently interrupted and the [11]CPP start to behave as an isolated entity (again this would be a kinetically blocked state in the solid after thermal template).

As for the C_{70} bands is concerned, temperature scarcely affects them by –1 cm^{-1} in all cases in the range of temperature analyzed, an observation that contrasts with their significant changes in the pressure experiments.

G Structural responses of the [9]- and [12]CPP@C_{70} complexes under mechanical and thermal stresses.

Figure 9 displays the Raman spectra of [9]CPP@C_{70} under pressure. Given the small volume of the innermost cavity of [9]CPP, we have inferred from the Raman changes in the complex, on the formation of a species of proto-complex. The Raman spectrum of [9]CPP@C_{70} as a function of pressure in the initial stages of the compression displays the typical frequency upshift inherent to the increment of intermolecular contacts; however, at around ≈2 GPa, the spectrum evolves by showing a dominant low frequency component at 1579 cm^{-1} together with another feature at 1604 cm^{-1}. These changes at high pressure persist after pressure release, the G bands downshift 2 cm^{-1}, what might be interpreted by arguing that the application of pressure further helps the formation of the supramolecular complex, a compound that it is not formed directly from solution. Nonetheless, the binary system formed from solution is in a suitable disposition to progress with pressure towards the final complex where, likely, the [9]CPP more effectively surround the corannulene fragments of the fullerene.

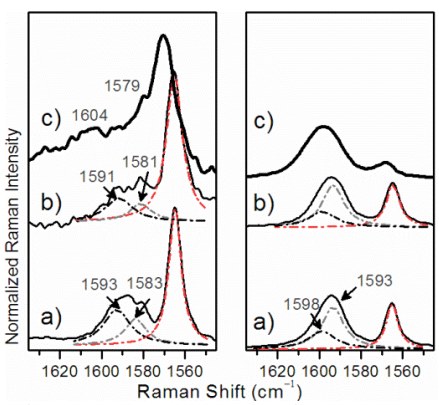

Figure 9. Left: 785 nm Raman spectra of [9]CPP@C_{70}: a) at room temperature and pressure; b) black line corresponds to the spectrum at high pressure (≈ 2.0 GPa); and c) the recovered spectrum after pressure cycle. Both spectra taken at 25 ºC. Dashed lines correspond to the deconvoluted bands. Right: the same for [12]CPP@C_{70}.

In the case of [12]CPP@C_{70}, the increment of pressure up to ≈2 GPa scarcely affects the frequencies of cycloparaphenylene unit, likely due to the moderate pressure increment. Again the largest changes are detected for the fullerene bands in agreement with these molecular entities supporting the transmission of the mechanical stress.

F Conclusions.

The electronic and structural properties of host-guest supramolecular 1:1 complexes of [n]CPPs and C_{70}, [n]CPP@C_{70} with n=9,10, 11 and 12, have been thoroughly analyzed by using Raman spectroscopy. We have found that the vibrational Raman spectra, and in particular the bands associated with the CC stretching tangential G modes and with the radial breathing modes of both [n]CPP and C_{70}, contain the relevant electronic and structural information resulting from complexation. Depending on their sizes, the [n]CPPs have been shown to be able to adapt their structures to form stable couplings with C_{70}: in [10]CPP@C_{70} the fullerene is surrounded by the [10]CPP by its equatorial part, or lying orientation, a situation that we now further characterize as having less staggered structure for the CPP. In [11]CPP@C_{70} the fullerene is wrapped up through its long ellipsoidal axis, or standing orientation, where the nanoring gets ovallized with close contacts in the C_{70} poles and less conformational restriction in the flattened region.

Under mechanical stress, the largest frequency changes are found for the fullerene bands revealing that the [n]CPPs, as for the unit cell of the solid is concerned, occupy the empty spaces, with the C_{70} molecules in the prevalent sites. In addition, pressure produces the modification of the lying structure of the [10]CPP@C_{70} complex towards a more standing-like shape followed by the flattening of its structure, a dual process that overall renders an irreversible structural mechanical cycle. [11]CPP@C_{70}, however, resists in its standing position by applying pressure, and it is by heating that the CPP ring seems to rotate towards a lying disposition by finally recovering its "isolated" spherical aspect. All in all, these data display the great adaptability of the [n]CPPs to the shape of C_{70} and also to the crystalline structure in the fullerene solid. C_{70} molecules are encapsulated in SWCNTs forming the well-known peapods where the fullerene molecules might adopt both lying and standing positions existing in many cases as mixtures of both. Here in the analysis of the [n]CPP as models of SWCNTs, the characterization by Raman of these well-defined complexes might help to understand the complexity of these peapods between fullerene and SWCNT.

The main message of this study is the impressive structural versatility and adaptability of the [n]CPP molecules to different physico-chemical environments, a chameleon-like property provided by the conjunction of unusual effects as cyclic conjugation and ring strain cylindrical shape which forms a delicate ground electronic state equilibrium easily modifiable through external physical and chemical inputs.

Notes and references

[a]*Department of Physical Chemistry, University of Málaga, CEI Andalucía Tech, Campus de Teatinos s/n, 29071-Málaga, Spain. Fax: 0034952132000; Tel: 0034952131868; E-mail: casado@uma.es*

Finantial support from MINECO of Spain, CTQ2012-33733, CTQ2012-38599-C02-02, CSD2007-00045, Junta de Andalucía (Project P09-FQM-4708) and Comunidad de Madrid (S2009/PPQ-1551) are acknowledged. M.P.A. is grateful to the Spanish MEC for an FPU grant.

1 V.C. Parekh and P.C. Guha, *J. Indian Chem. Soc.*, 1934, **11**, 95.

2 R. Jasti, J. Chattacharjee, J. B. Neaton and C.R. Bertozzi, *J. Am. Chem. Soc.*, 2008, **130**, 17646.

3 H. Omachi, S. Matsuura, Y. Segawa and K. Itami, *Angew. Chem. Int. Ed.*, 2010, **49**, 10202; H. Takaba, H. Omachi, Y. Yamamoto, J. Bouffard and K. Itami, *Angew. Chem. Int. Ed.*, 2009, **48**, 6112; Y. Segawa, S. Miyamoto, H. Omachi, S. Matsuura, P. Senel, T. Sasamori, N. Tokitoh and K. Itami, *Angew. Chem. Int. Ed.*, 2011, **50**, 3244; H. Omachi, Y. Segawa and K. Itami, *Acc. Chem. Res.*, 2012, **45**, 1378; Y. Ishii, Y.Nakanishi, H. Omachi, S. Matsuura, K. Matsui, H. Shinohara, Y. Segawa and K. Itami, *Chem. Sci.*, 2012, **3**, 2340.

4 E. Kayahara, T. Kouyama, T. Kato, H.Takaya, N. Yasuda and S. Yamago, *Angew. Chem. Int. Ed.*, 2013, **52**, 13722; T. Iwamoto, Y. Watanabe, Y. Sakamoto, T. Suzuki and S. Yamago, *J. Am. Chem. Soc.*, 2011, **133**, 8354; S. Yamago, Y. Watanabe, T. Iwamoto, *Angew. Chem. Int. Ed.*, 2010, **49**, 757; E. Kayahara, Y. Sakamoto, T. Suzuki and S. Yamago, *Org. Lett.*, 2012, **14**, 3284.

5 J. Xia and R. Jasti, *Angew. Chem. Int. Ed.*, 2012, **51**, 2474; T. J. Sisto, M. R. Golder, E. S. Hirst and R. Jasti, *J. Am. Chem. Soc.*, 2011, **133**, 15800; T. J. Sisto and R. Jasti, *SynLett.*, 2012, **23**, 483; E. S. Hirst and R. Jasti, *J. Org. Chem.*, 2012, **77**, 10473; R. Jasti, C. R. Bertozzi, *Chem. Phys. Lett*., 2010, **494**, 1; J. Xia, J. W. Bacon and R. Jasti, *Chem. Sci.*, 2012, **3**, 3018; M. R. Golder, B. M. Wong and R. Jasti, *Chem. Sci*., 2013, **4**, 4285; A. V. Zabula, A. S. Filatov, J. Xia, R. Jasti and. M.A. Petrukhina, *Angew. Chem. Int. Ed.*, 2013, **52**, 5033.

6 E. Kayahara, V. K. Patel and S. Yamago, *J. Am. Chem. Soc*.,2014, **136**, 2284; P. J. Evans, E. R. Darzi and R. Jasti, *Nat. Chem.*, 2014, **6**, 404.

7 H. Omachi, T. Nakayama, E. Takahashi, Y. Segawa and K. Itami, *Nat. Chem.*, 2013, **5**, 572.

8 Y. Segawa, H. Omachi and K. Itami, *Org. Lett.*, 2010, **12**, 2262.

9 See papers in references 2-5 where the molecular structures of some [n]CPPs are resolved by x-ray diffraction. In addition: S. Taubert, D. Sundholm and F. Pichierri, *J. Org. Chem*., 2010, **75**, 5867; U. H. F. Bunz, S. Menning and N. Martín, *Angew. Chem. Int. Ed.*, 2012, **51**, 7094; S. Schrettl and H. Frauenrath, *Angew. Chem. Int. Ed.*, 2012, **51**, 6569.

10 T. Iwamoto, Y. Watanabe, T. Sadahiro, T. Haino and S. Yamago, *Angew. Chem. Int. Ed.*, 2011, **50**, 8342.

11 M. Peña Alvarez, P. Mayorga Burrezo, M. Kertesz, T. Iwamoto, S. Yamago, J. Xia, R.Jasti, J. T. López Navarrete, M. Taravillo, V. G. Baonza and J. Casado, *Angew. Chem. Int. Ed.*, DOI: anie.201400719.

12 T. Iwamoto, Y. Watanabe, H. Takaya, T. Haino, N. Yasuda and S. Yamago, *Chem. Eur. J*., 2013, **19**, 14061.

13 V. G. Baonza, M. Taravillo, A. Arencibia, M. Cáceres and J. Núñez, *J. Raman Spectrosc.* 2003**, 34**, 264.

14 E. del Corro, J. González, M. Taravillo, E. Flahaut and V. G. Baonza, *Nano Lett*., 2008, **8**, 221516.

15 G. Sun and M. Kertesz, *J. Phys. Chem. A*, 2002, **106**, 6381. V. Schettino, M. Pagliai, G. Cardini, H. *J. Phys. Chem. A*, 2002, **106**, 1815. D. Jing, Z. Pan, *Eur. J. Mech. A/Sol*., 2009, **28**, 948.

16 S. Tsuzuki, K. Honda, T.Uchimaru, M. Mikami, k. Tanabe, . *Am. Chem. Soc*., 2002, **124**, 104-112.

17 C. Caillier, D. Machon, A. San-Mighel, R. Arenal, G. Montagnac, H. Cardon, M. Kalbac, M. Zukalova, L. Kavan, *Phys Rev. B*, 2008, **77**, 125418.

18 P. M. Rafailov, C. Thomsen, H. Kataura, *Phys. Rev. B*, 2003, **68**, 193411; A.N. Khlobystov, R. Scipioni, D. Nguyen-Manh, D. A. Britz, D. G. Pettifor, G. A. D. Briggs, S. G. Lyapin, A. Ardavan, R. J. Nicholas, *Appl. Phys. Let.*, 2004, **84**, 772.